ST-Segment Alterations in the Electrocardiogram of Acute Pulmonary Thromboembolism: A Rabbit Model

Dongchao LIU[1], Bing DUAN[1], Meina Zhao[1], Lin Wu[1], Yazhen Cao[1], Ningbo Liu[1], Zheng Xue[1], ZhiHong He[2], Jie Mi[1]

[1]Department of cardiology, Shijiazhuang People's Hospital, Heibei Province, China, [2]Department of emergency medicine, Shijiazhuang People's Hospital, Hebei Province, China

Received October 24, 2023
Accepted February 29, 2024

Summary

In this study, we investigated the mechanism underlying electrocardiogram (ECG) alterations in a rabbit model of acute pulmonary thromboembolism (PTE). Twelve healthy adult New Zealand white rabbits were used, with eight in the experimental group (PTE group) and four in the control group. After developing the rabbit model of acute PTE, ECG and coronary angiography were performed. HE staining was conducted on the right and left ventricular tissues, and polymerase chain reaction (PCR) was used to determine brain natriuretic peptide (BNP), tumor necrosis factor-alpha (TNF-α), and Troponin I (TNI) mRNA expression in the myocardium. There were considerable changes in the ST segment of the ECG in the PTE group. Coronary angiography revealed the absence of spasm, stenosis, and occlusion. In the plasma of the PTE group, the levels of D-dimer, BNP, TNF-α, and TNI were significantly elevated, and these changes were statistically significant ($P<0.05$). PCR analysis of ventricular myocardial tissue indicated significantly higher levels of BNP, TNF-α, and TNI mRNA in the PTE group than in the control group. These differences were statistically significant ($P<0.05$). The ST-T variations on the ECG of rabbits with acute PTE correlate strongly with the temporary changes in right heart volume caused by acute PTE.

Keywords: Animal model of pulmonary embolism • B-type natriuretic peptide • Electrocardiogram • Pulmonary thromboembolism • Troponin I • Tumor necrosis factor-α.

Corresponding author

Jie Mi, Department of cardiology, Shijiazhuang People's Hospital, 365 Jianhua South Street, Yuhua District, Shijiazhuang City, Hebei Province 050000, China. Email: jeremymijie@126.com; ZhiHong He, Department of emergency medicine, Shijiazhuang People's Hospital, 365 Jianhua South Street, Yuhua District, Shijiazhuang City, Hebei Province 050000, China. Email: hezhihonghezh@126.com

Introduction

Pulmonary thromboembolism (PTE) is delineated by the obstruction of the pulmonary artery or its branches, consequent to a thrombus originating either from a venous source or the right cardiac system. Such occlusion culminates in compromised pulmonary circulation and respiratory aberrations, which emerge as the cardinal clinical presentations of the condition. It has an elevated incidence, frequent misdiagnoses, and significant mortality rate, placing it prominently among the principal causative agents of cardiovascular-related fatalities [1]. Concurrently, the onset of pulmonary embolism (PE) frequently induces electrocardiogram (ECG) alterations, predominantly typified as $S_IQ_{III}T_{III}$, in tandem with elevations or depressions in the ST-segment [2]. The precise etiological mechanism of this condition remains unclear. Some postulate that it arises due to right cardiac dilation as a consequence of augmented pulmonary arterial pressure. Contrarily, certain academicians posit that it may be attributed to ephemeral coronary spasms or myocardial infarction. A few even conjecture its origin to be the migration of the embolus to the left cardiac system via an unsealed patent foramen ovale (PFO), which subsequently proceeds into the coronary arterial system post-PTE, eliciting elevated pressures within the right

heart [3]. Some studies have shown that brain natriuretic peptide (BNP), tumor necrosis factor-alpha (TNF-α), Troponin I (TNI) and other biomarkers can reflect changes in heart and pulmonary embolism[4,5], and these parameter changes may be related to ST segment alterations in the electrocardiogram. As such, our endeavor is to emulate this sequence through animal-based experimentation to elucidate the transformations in the circulatory dynamics and myocardial trauma. The objective is to enhance prevailing diagnostic and therapeutic methods.

Materials and Methods

Laboratory Animals

In this study, a cohort of 12 healthy adult New Zealand White rabbits, each weighing between 2.5 to 3.0 kg, were procured from the Xinglong Experimental Animal Breeding Farm located in Haidian District, Beijing. These male rabbits bore a licensure identifier of SCXK (Beijing) 2011-0009. For differentiation, each rabbit was digitally labeled on the forehead. Subsequently, they were assorted in a 2:1 proportion and were arbitrarily allocated to either the PTE group or the control group. The former comprised 8 rabbits, and the latter constituted 4 rabbits. Prior to any surgical intervention, the rabbits were acclimatized to their new surroundings for a minimum duration of one week. Their habitat was facilitated by the Animal Experimentation Center at TEDA International Cardiovascular Disease Hospital. Environmental parameters were meticulously controlled with the room temperature maintained at 24°C and a relative humidity of 40 %. The dietary feed for the rabbits was procured concomitantly with the animals from the aforementioned breeding farm.

Methods

Establishment of PTE animal model

Rabbits assigned to the PTE group underwent a fasting period of 12 hours before surgical intervention. A 24-gauge cannulated needle was used to puncture the marginal ear vein, which was then secured using tape and prepped by flushing heparin saline.

General Anesthesia induction was achieved with a 30 mg/kg intravenous dose of 3 % pentobarbital sodium at the ear margin. During the procedure, if signs of agitation were observed, an additional 5 mg/kg was administered. Subsequent to the immobilization of the limbs of the rabbit, the animal was laid in a supine position and fastened to the surgical table.

Electrodes were affixed to the prepared skin of the limbs and the thoracic center, then connected to a Datex-Ohmeda 7000 electrocardiographic monitor. ECG limb leads, along with the V1 lead, were connected using a large head pin. Following skin preparation on the neck, routine iodophor disinfection, area draping, and lidocaine-induced local anesthesia, a longitudinal incision of approximately 2-2.5 cm was established on the right side of the trachea. The jugular vein was methodically isolated. The use of lidocaine is to simulate real vascular puncture procedures while minimizing any potential complications caused by vascular puncture itself. Concurrently, to prevent potential asphyxiation, the tongue was outwardly extended.

The Seldinger vascular puncture technique was used. Upon successful puncture of the jugular vein using a 20-gauge cannula needle, the core was excised. A contrast agent was used to confirm the correct jugular vein lumen positioning. The radial artery facilitated the guide wire's path to the inferior vena cava. After removing the cannula, a 4F sheath tube was navigated along the guide wire into the right atrium. Blood (1 mL) was then drawn from this tube, left at ambient temperature for clotting, and subsequently heated in a 70 °C water bath for 10 minutes.

A parallel incision was made on the left side of the trachea to access the carotid artery. After puncturing the artery, the needle core was removed and a guide wire was navigated to the root of the aorta. A 4F sheath tube was inserted into the ascending aorta for arterial blood extraction and gas analysis. A pigtail catheter was used to examine potential stenosis or occlusion in the coronary arteries.

A loach guidewire was navigated through the right sheath and into the pulmonary artery. A 4F pigtail catheter was directed along the guidewire into the right ventricle. With the catheter tip anchored to the pulmonary valve, pulmonary arteriography was conducted in three orientations: posterior-anterior (Fig. 1A), left anterior oblique (Fig. 1B), and right anterior oblique (Fig. 1C). Subsequently, pulmonary artery pressures were recorded.

Three cylindrical autologous blood clots were injected through the pigtail catheter, followed by a 10 ml saline flush, embedding the clots in the pulmonary artery. Post-procedure, ECG and pulmonary arteriography were performed using earlier described positions. Pulmonary artery blood flow was assessed and continuous

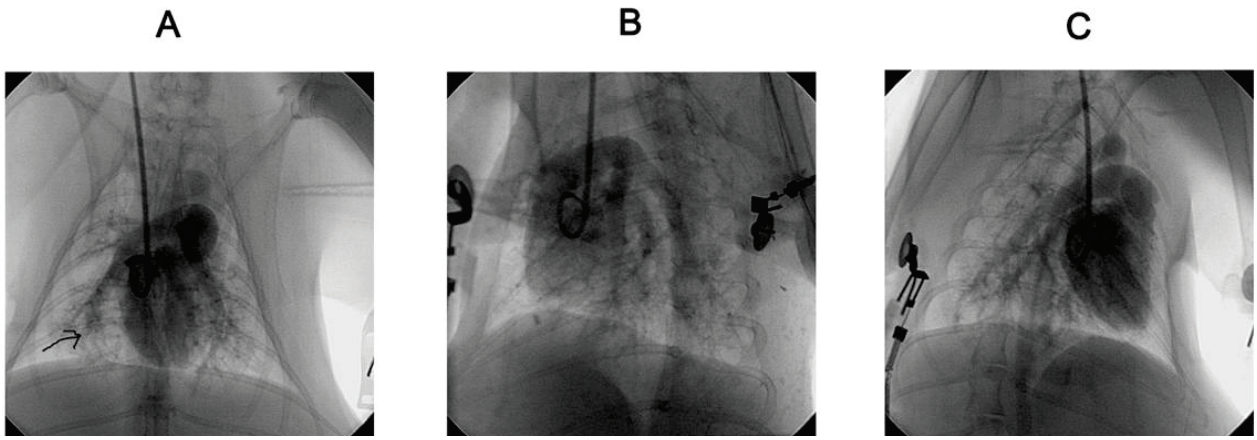

Fig. 1. A) posterior anterior position; **B)** left anterior oblique position; **C)** right anterior oblique position

monitoring of pressures was maintained. Arterial blood was sampled from the left carotid for blood gas analysis and non-selective angiography verified coronary artery status.

The rabbits were euthanized 2 hours post-modeling using a 100 mg/kg dose of 3 % pentobarbital sodium. Lungs were swiftly excised, preserved in 10 % formaldehyde, and subsequently stained with HE for histological evaluation. All specimens were processed for analysis within the same day to ensure uniformity.

Modeling of experimental rabbits in the control group

For the control group, the procedural methodology paralleled that of the PTE group. Specifically, vascular accesses were established *via* the right jugular vein and the left carotid artery. However, diverging from the PTE group, only a 10 ml saline solution was injected into the pulmonary artery using the pigtail catheter, with the conspicuous absence of any autologous thrombus. Subsequent to the modeling process, assessments encompassing ECG, pulmonary arteriography, coronary arteriography, and a repeated blood gas analysis were undertaken. For further evaluation, macroscopic tissue specimens were preserved.

Blood gas analysis

Following the placement of the sheath tube into the carotid artery and the execution of the pulmonary artery thromboembolism procedure, 1 ml of blood specimen was procured from the carotid artery sheath tube using a BD arterial blood collection tube. This sample was subsequently assessed with the NOVA Biomedical STAT PROFILE M blood gas analyzer. Parameters of the blood gas analysis encompassed Pondus Hydrogenii (pH), partial pressure of carbon dioxide (PCO_2), partial pressure of oxygen (PO_2) among others.

HE staining

Post-euthanasia, cardiac tissues from the rabbits were excised and promptly placed in a 10 % formaldehyde solution for fixation. Within a week, these specimens were retrieved, subjected to a dehydration process, clarified, immersed in wax, and subsequently embedded to form paraffin blocks for future histological analyses.

Sections from these paraffin blocks were sliced to a thickness of 5 μm and affixed to Poly-D-lysine-treated APS-coated glass slides. The standard deparaffinization procedure was employed, which involved rehydration of the sections. The slides were then stained using Harris hematoxylin for a duration of 5 minutes, followed by a thorough water rinse lasting 3 minutes. Subsequently, the sections were differentiated in an ethanol hydrochloric acid solution for 30 seconds. After a 1-minute water rinse, the sections were treated with an ammonia solution to achieve blue counterstaining for 30 seconds, followed by another 3-minute water rinse. The tissue sections were then stained with eosin for approximately 2–3 minutes and briefly rinsed in tap water. A gradient alcohol series was used for dehydration, after which the sections were cleared using xylene. Ultimately, the sections were mounted and sealed with neutral gum for microscopic examination.

Utilizing an Olympus microscope at 10× magnification, structural and organizational alterations in both the left and right cardiac sections were meticulously examined. Representative images capturing typical views of the observed changes were then selected.

Determination of D-dimer, BNP, TNF-α, and TNI in plasma

Blood samples, amounting to 2.7 mL each, were procured from the right jugular vein and left carotid artery of the experimental rabbits at three distinct time points: prior to the modeling procedure and at intervals of 1–2 hours post-modeling. Following extraction, the samples were transferred to anticoagulant test tubes, which contained 0.3 mL of a 0.19 mmol/L sodium citrate solution. After being thoroughly mixed, the samples underwent centrifugation at a speed of 3,000 rpm for a duration of 15 minutes. Subsequently, the plasma was isolated and preserved at a temperature of -80°C until further analysis. Upon the conclusion of the experimental phase, all plasma samples were consistently assessed utilizing the ELISA method.

Western blot analysis of BNP, TNF-α, and TNI in left and right ventricular myocardial tissues

For cell lysis, a total of 100 mg of tissue was subjected using 400 μl of RIPA lysate. The tissue underwent mechanical disruption using a tissue grinder and subsequently incubated on ice for a duration of 30 minutes. Periodic cell disruption was facilitated by pneumatic perturbation. Following the lysis procedure, the proteins were harvested and preserved at a temperature of -80°C. Proteins were separated using the SDS-PAGE gel electrophoresis technique. To assemble the separation gel for a 10 % SDS-PAGE gel, 32 μl of total protein was amalgamated with 8 μl of 5× loading buffer. The solution was subjected to boiling for 3 minutes, followed by an immediate cooling phase on ice for an additional 3 minutes. The sample was then loaded onto the gel, with electrophoresis being conducted at a consistent voltage of 100 V. Post-electrophoresis, proteins were translocated onto a nitrocellulose membrane (sourced from Millipore, USA) through electrophoretic transfer at 350 mA for a duration of 120 minutes at 4°C. The membrane was labeled for orientation—distinguishing the anterior from the posterior, as well as lateral demarcations. The membrane was then incubated in a Blotto blocking solution, undergoing gentle agitation at ambient temperature for approximately 1.5 hours. For antibody binding, the primary antibody was introduced to the membrane and left to bind overnight at 4°C, with continuous mild agitation. Any non-specifically adhered primary antibody was removed with three sequential washes in 1× TBST, each lasting five minutes. Subsequent to primary antibody binding, the membranes were immersed in a Blotto solution containing the HRP-conjugated goat anti-rabbit IgG secondary antibody. This binding step lasted 2 hours at room temperature with persistent gentle agitation. Post-binding, non-specific secondary antibodies were removed using a washing protocol similar to that employed for the primary antibodies. The protein bands were eventually detected using the Western Lightning®-ECL, an enhanced chemiluminescence substrate (sourced from Perkin Elmer, NEL100001EA). Documentation of the results was achieved using a specialized gel imaging system.

Determination of BNP, TNF-α, and TNI mRNA in left and right ventricular myocardial tissues

Quantitative analysis of BNP, TNF-α, and TNI mRNA expression using real-time fluorescence quantitative polymerase chain reaction (PCR) was conducted. Total RNA was isolated from the tissues employing conventional techniques. The integrity of the extracted RNA was subsequently validated through agarose gel electrophoresis. β-actin, served as the internal reference to normalize the expression levels. The genes of interest encompassed BNP, TNF-α, and TNI. Primer sequences specific to the CDS regions of BNP, TNF-α, and TNI were meticulously crafted using the Primer Premier 5.0 software, drawing from the available genetic data on these genes. For the reverse transcription process, 5 μg of the extracted RNA was subjected to MMLV reverse transcriptase (Catalogue Number: 9PIM170) and associated reagents. The reaction was facilitated in a total volume of 20 μl. For the qPCR, 0.5 μl of the resulting reverse transcription (RT) product was incorporated. The reaction mixture contained SYBR® Premix Ex TaqTM (sourced from TaKaRa). The thermocycling conditions were as follows:

Denaturation: 94°C for 30 seconds

Annealing: 50°C for 30 seconds

Extension: 72°C for 40 seconds

This 3-step cycling procedure was repeated over 40 cycles. Post-amplification, both the target gene amplifications and the β-actin were visualized under the KODAK gel imaging system. The results were documented, and a DNA ladder served as the molecular weight reference during gel electrophoresis. This experimental procedure provides a quantitative assessment of BNP, TNF-α, and TNI mRNA expression levels, leveraging the precision of real-time fluorescence quantitative PCR.

Statistical methods

All the data were entered into an Access database, and SPSS 17.0 software was used for statistical analysis. The measurement data are expressed as mean ± standard deviation. The comparison of data between the PTE group and control group was conducted using an independent samples *t*-test. A paired *t*-test was used for comparing the data before and after modeling within the PTE group and control group. In addition, $P<0.05$ was considered statistically significant.

Result

PTE animal model and coronary angiography results

The PTE model was 100 % successfully modeled in this group of rabbits. After receiving the bolus injection, the rabbits in the PTE group developed symptoms and signs including shortness of breath, restlessness, cyanosis of the lips and mouth, and an increased heart rate. Pulmonary arteriography revealed right ventricular enlargement, pulmonary artery thickness, and filling deficiencies, truncation, or complete absence. The ECG revealed considerable alterations to the ST segment (Fig. 2A, Fig. 2B). Coronary angiography indicated no spasm, stenosis, or blockage of the coronary arteries.

HE staining results

In both the experimental and control groups, HE staining of the left ventricle revealed no anomalies in the myocardial structure, normal cell arrangement, or inflammatory cell infiltration. The HE staining results of the right ventricle revealed that both the PTE and control groups had normal myocardial structure and cell organization. No inflammatory cell infiltration was detected, and neither group displayed any evident abnormalities (Fig. 3).

ELISA Results

D-Dimer Results

In the PTE group, D-Dimer levels were observed to be raised 1–2 hours following PTE modeling. This difference was statistically significant when compared to the levels before modeling ($P<0.05$) and to the control group ($P<0.05$). D-Dimer levels were marginally elevated in the control group 1 and 2 hours after modeling, and the difference was statistically significant ($P<0.05$) compared to the PTE group (Table 1).

BNP Results

In the PTE group, BNP levels were elevated 1 hour and 2 hours after PTE modeling. These differences were statistically significant compared to both the pre-modeling period and the control group ($P<0.05$). At 1 and 2 hours following the modeling, there was also a modest increase in BNP levels in the control group, and this difference was statistically significant when compared to the PTE group ($P<0.05$) (Table 2).

TNF-α and TNI Results

In the PTE group, TNF-α and TNI levels were elevated 1 hour and 2 hours after PTE modeling. These differences were statistically significant in comparison to both the pre-modeling period ($P<0.05$) and the control group ($P<0.05$). Statistically, there was no difference between the control group before and after modeling (Tables 3 and 4).

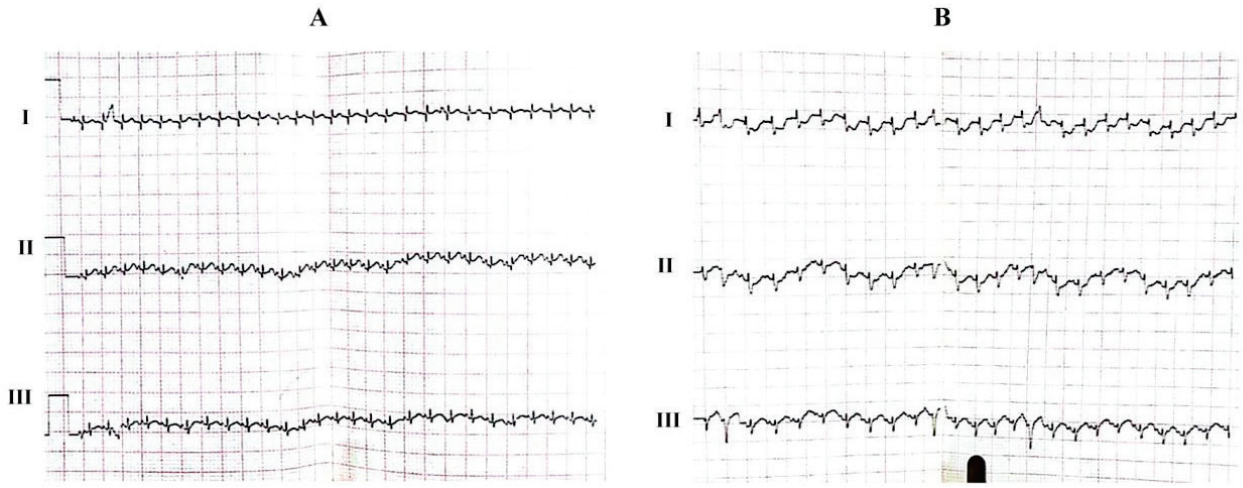

Fig. 2. A) Pre-modeling ECG, no ST-T changes were observed; **B)** Post-modeling ECG, obvious ST-T changes were observed

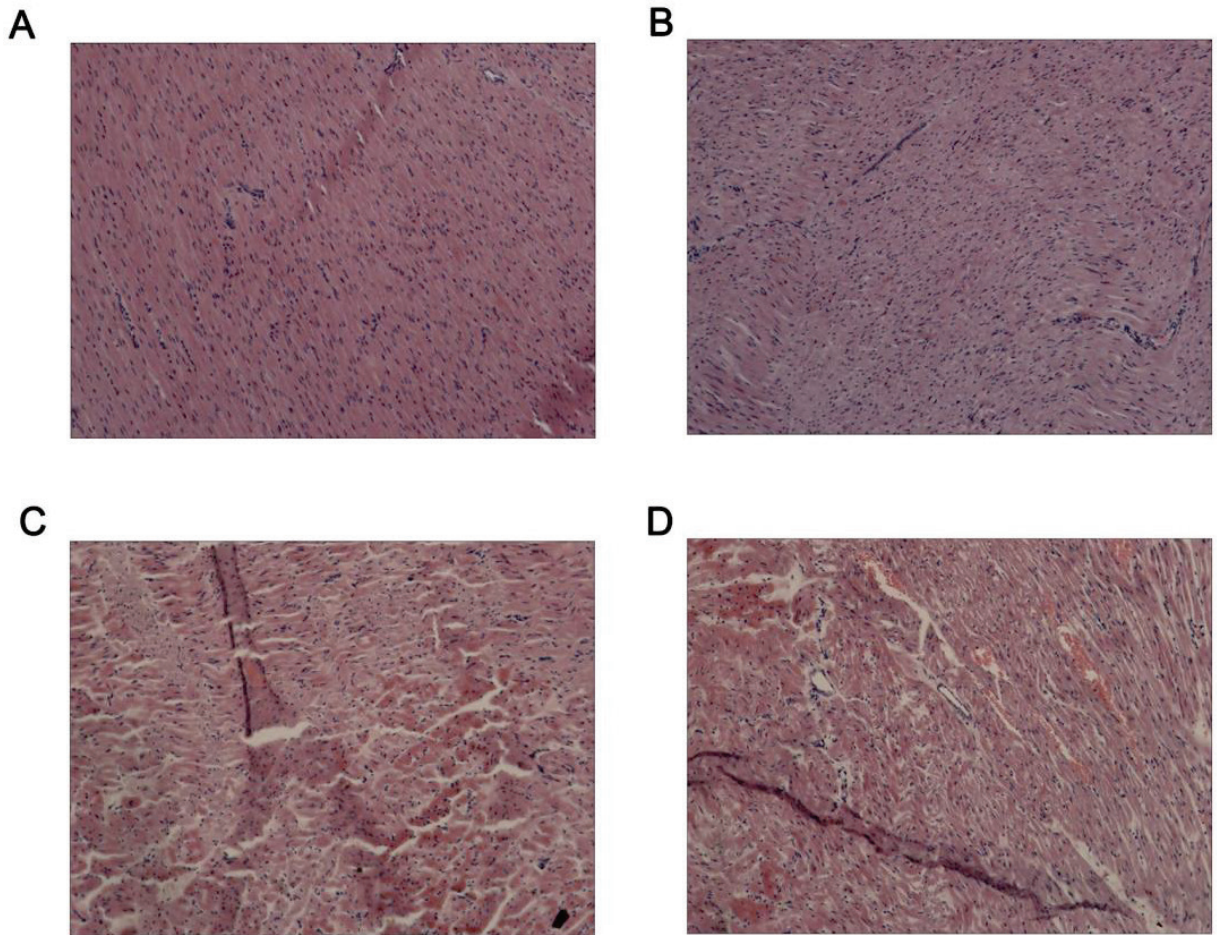

Fig. 3. HE staining of left and right ventricular myocardial tissue after modeling in different groups of experimental rabbits (×10). **A)** The left heart tissue sections of the experimental group, **B)** Left heart tissue sections of the control group, **C)** Right heart tissue sections of the experimental group, **D)** Right heart tissue sections of the control group

Table 1. Comparison of D-Dimer prior to and subsequent to PTE modeling (ng/ml)

Time	Control group	PTE group	*P*
Prior to modeling	321.21±20.19	311.20±24.08	0.456
1 hour post modeling	364.74±29.60*	643.57±34.52*	<0.001
2 hours post modeling	372.53±31.43*	660.88±30.53*	<0.001

* The difference was statistically significant when compared with the control group (P<0.05);

Table 2. Comparison of BNP before and after PTE modeling (pg/ml)

Time	Control group	PTE group	*P*
Prior to modeling	50.51±1.74	52.51±5.07	0.454
1 hour post modeling	59.20±4.73*	96.19±11.49*	<0.001
2 hours post modeling	64.54±10.24*	105.93±7.42*	<0.001

* The difference was statistically significant when compared with the control group (P<0.05);

Table 3. Comparison of TNI before and after PTE modeling (pg/ml)

Time	Control group	PTE group	*P*
Prior to modeling	117.77±18.63	109.02±22.26	0.480
1 hour post modeling	119.01±17.84	192.34±19.29	<0.001
2 hours post modeling	119.95±18.34	207.16±10.98	<0.001

Table 4. Comparison of TNF-α before and after PTE modeling (pg/ml)

Time	Control group	PTE group	*P*
Prior to modeling	39.46±7.12	36.20±8.44	0.487
1 hour post modeling	45.89±4.53	75.75±11.37	<0.001
2 hours post modeling	48.34±10.09	88.13±9.07	<0.001

Determination of BNP, TNF-α, and TNI via western blot in left and right ventricular myocardial tissue

BNP, TNF-α, and TNI protein expression was elevated in the left and right ventricular myocardial tissues of the PTE group, and the difference was statistically significant (P<0.001) when compared to the control group (Figs 4A and 4B).

Determination of BNP, TNF-α, and TNI mRNA in left and right ventricular myocardial tissues

The expression levels of BNP, TNF-α, and TNI mRNA in the left and right ventricular myocardial tissues of the PTE group were elevated, and the difference was statistically significant compared to those of the control group (P<0.001) (Figs 5A and 5B).

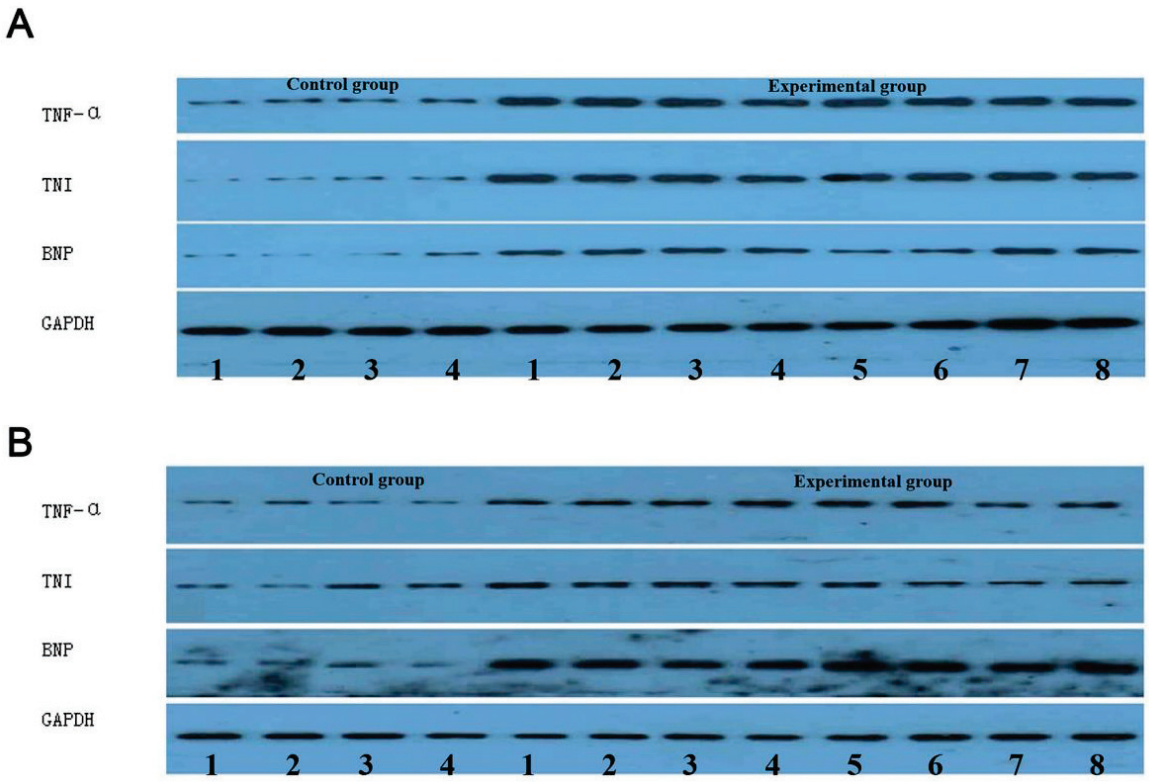

Fig. 4. A) Comparison of BNP, TNF-α, and TNI WB results in right ventricular myocardial tissue after modeling in different groups of experimental rabbits; **B)** Comparison of BNP, TNF-α, and TNI WB results in left ventricular myocardial tissue after modeling in different groups of experimental rabbits

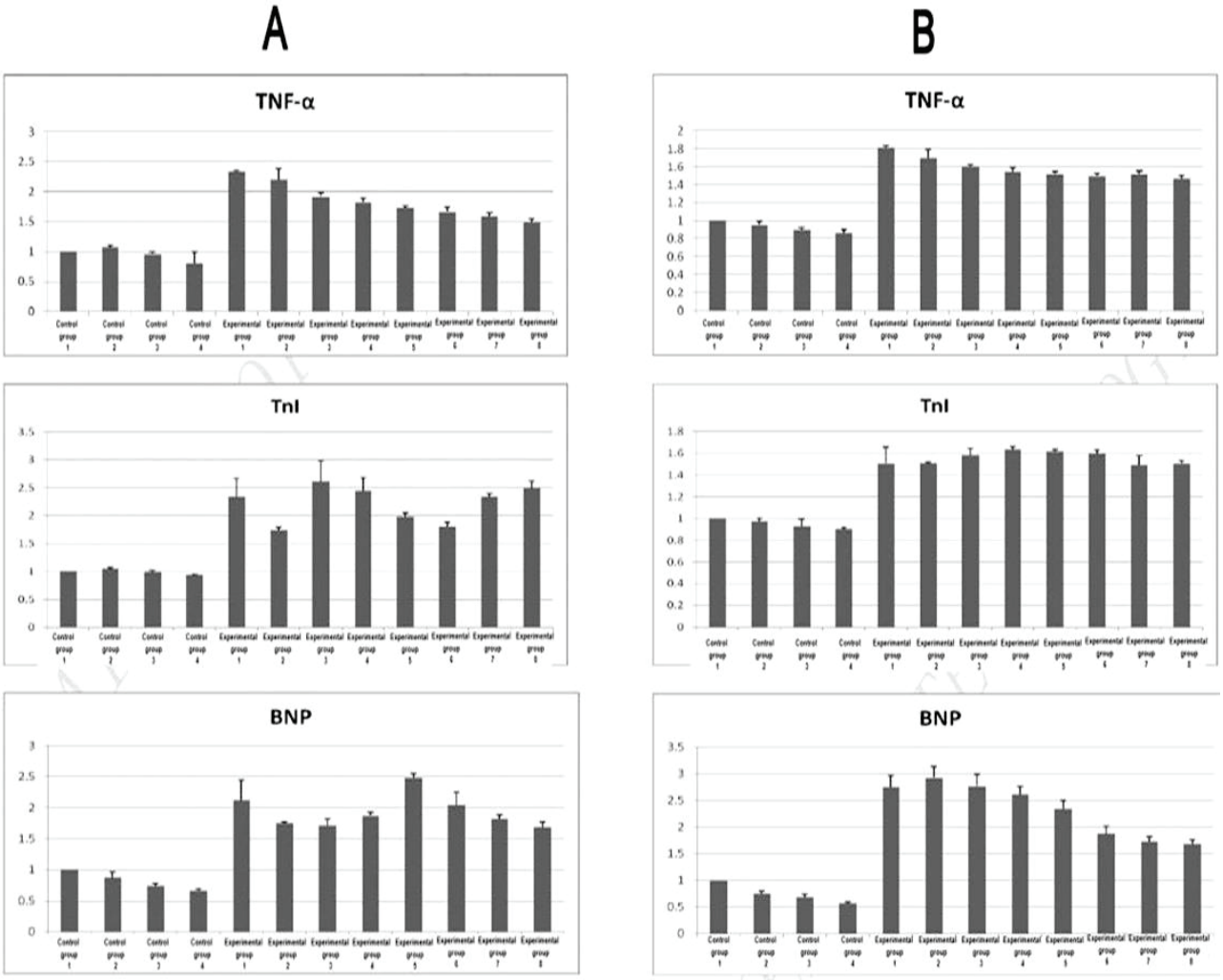

Fig. 5. A) Comparison of BNP, TNF-α, and TNI mRNA expression levels in left ventricular myocardial tissues after modeling of experimental rabbits in different groups; **B)** Comparison of BNP, TNF-α, and TNI mRNA expression levels in right ventricular myocardial tissues after modeling of experimental rabbits in different groups.

Discussion

PTE is a vascular obstruction primarily caused by thrombi originating from veins or the right cardiac system. This obstruction culminates in compromised pulmonary circulation and respiratory abnormalities. Notably, PTE is a significant concern in cardiovascular diseases due to its high incidence, diagnostic challenges, and mortality rate [1]. According to the study, patients with different degrees of pulmonary embolism may exhibit different ECG presentations. Some scholars have investigated the value of ECG in risk stratification for PTE [6-8].

ECGs have been instrumental in understanding the cardiovascular impacts of PTEs. Distinct ECG deviations, including the $S_IQ_{III}T_{III}$ syndrome and sinus tachycardia, are frequently associated with acute PTE [9,10]. Additionally, T-wave inversions, ST-segment alterations, atrial fibrillation, and clockwise rotation also typify the ECG landscape in PTE cases [11]. Despite these insights, the precise patho-physiology underlying ECG modifications in PTE remains under-researched. Our study involved the systematic induction of a PTE model in white rabbits, with all experimental animals manifesting significant ST-T changes on ECG. Concomitant coronary angiography ruled out coronary anomalies, suggesting these ECG modifications were not resultant of coronary lesions. Interestingly, right ventricular enlargement was discernible, a finding missing in the control animals. BNP, a cardiomyocyte-derived natriuretic peptide, gets upregulated during cardiac stress [12]. BNP level in the blood can directly reflect the right heart function and the degree of pulmonary embolism in patients [13]. In this study, elevated BNP levels

were corroborated post-PTE induction, aligning with increased cardiomyocyte stress [14]. Furthermore, elevations in pro-inflammatory cytokine TNF-α and cardiac injury marker TnI were evident, underlining the profound cardio-vascular ramifications of PTE [15]. However, traditional histological evaluations, such as HE staining, failed to elucidate overt myocardial damage. This paradox warrants microscopic evaluations to potentially unveil cardiomyocyte apoptosis.

Historically, ECG ST-T deviations in PTE have been ambiguously linked to coronary events [16,17]. Our findings challenge this notion, contending that post-PTE hemodynamic alterations—chiefly rising pulmonary artery resistance and ensuing ventricular dilations—underpin these changes in ECG [18]. In essence, acute PTE-induced ECG variations may be more attributable to cardiac volumetric changes than transient coronary incidents.

This study has a few limitations. Relying largely on retrospective data, coupled with a limited sample size, potentially curtails the robustness of the findings. In the future, there is a pressing need for expansive, prospective studies to further harness the potential of ECG in diagnosing and managing PTE.

Conclusion

Coronary angiography revealed that the ST-T alterations found in the rabbit model of acute PTE were not directly linked with occlusion, stenosis, or transient spasm of the coronary arteries. It may be closely associated with the transitory alterations in right heart volume brought about by acute PE. Through a thorough comprehension of this mechanism, we can enhance ECG application scenarios for the diagnosis and treatment of patients with acute PE. This will increase the knowledge and comprehension of ECG in pulmonary embolism physicians, offering convenience for physicians and lowering the economic costs for patients.

Ethical approval

All experiments were evaluated and approved by the ethics Committee of Teda International Cardiovascular Hospital (TICH-A2012-1121-1) and complied with the National Institutes of Health Guide for the Care and Use of Laboratory Animals.

Conflict of Interest

There is no conflict of interest.

Acknowledgements

No external funding received to conduct this study.
We would like to acknowledge the hard and dedicated work of all the staff that implemented the intervention and evaluation components of the study.

References

1. Jaff MR, McMurtry MS, Archer SL, et al. Management of massive and submassive pulmonary embolism, iliofemoral deep vein thrombosis, and chronic thromboembolic pulmonary hypertension: a scientific statement from the American Heart Association. Circulation 2011;123:1788-1830. https://doi.org/10.1161/CIR.0b013e318214914f
2. Tomcsányi J, Turi-Kováts N, Wettstein A, Arabadzisz H. Massive pulmonary embolism causing large T-wave inversion and QT prolongation. Thorac Dis 2017;9:4671-4673. https://doi.org/10.21037/jtd.2017.10.89
3. Wąsek WC, Samul W, Ryczek R, et al. Unique case of ST-segment-elevation myocardial infarction related to paradoxical embolization and simultaneous pulmonary embolization: clinical considerations on indications for patent foramen ovale closure in no-guidelines land. Circulation 2015;131:1214-1223. https://doi.org/10.1161/CIRCULATIONAHA.114.009846
4. Zhou G, Xie D, Fan R, Yang Z, Du J, Mai S, Xie L, Wang Q, Mai T, Han Y, Lai F. Comparison of pulmonary and extrapulmonary models of sepsis-associated acute lung injury. Physiol Res 2023;72:741-752. https://doi.org/10.33549/physiolres.935123
5. Xia Y, Zhang W, He K, Bai L, Miao Y, Liu B, Zhang X, Jin S, Wu Y. Hydrogen sulfide alleviates lipopolysaccharide-induced myocardial injury through TLR4-NLRP3 pathway. Physiol Res 2023;72:15-25. https://doi.org/10.33549/physiolres.934928

6. Casazza F, Pacchetti I, Rulli E, et al. Prognostic significance of electrocardiogram at presentation in patients with pulmonary embolism of different severity. Thromb Res 2018;163:123-127. https://doi.org/10.1016/j.thromres.2018.01.025
7. Sirbu IV, Nistor DO, Hutanu A, et al. Can the electrocardiogram be used for predicting risk in patients with acute pulmonary embolism? Thromb Res 2018;166:76. https://doi.org/10.1016/j.thromres.2018.04.014
8. Qu CF, Wang GF. The significance of electrocardiogram in early risk stratification of patients with acute pulmonary embolism (in Chinese). Chinese J Gerontol 2019;39(20):4887-4889.
9. Chan TC, Vilke GM, Pollack M, et al. Electrocardiographic manifestations of pulmonary embolism. JEM 2001;21: 263-270. https://doi.org/10.1016/S0736-4679(01)00389-4
10. Bakebe A, Kashongwe I, Mulenga C, Tshiasuma M, Kabengele B, Bisuta SF, Makulo JR, Kashongwe Z, Kayembe J-M. Pulmonary embolism: epidemiological data and diagnosis in Kinshasa hospitals. Int J Tuberc Lung Dis 2017;21(8): 875-879. https://doi.org/10.5588/ijtld.16.0418
11. Gong XJ. Clinical value of combined echocardiography and electrocardiogram in the diagnosis of acute pulmonary embolism (in Chinese). China Health Care Nutrition 2019;29:24-28.
12. Chen YX, Li M, Chen XX, et al. Clinical value of measuring NT-proBNP, D-dimer and Fib plasma level in chronic obstructive pulmonary disease patients with pulmonary embolism. Hainan Med J 2017; 28:23-25.
13. Park JS, Ahn J, Choi JH, et al. The predictive value of echocardiography for chronic thromboembolic pulmonary hypertension after acute pulmonary embolism in Korea. Korean H Intern Med 2017;32:85-94. https://doi.org/10.3904/kjim.2014.175
14. Jian N, Tan LL, Wang MS, et al. Electrocardiogram changes in 72 cases of acute pulmonary embolism and their impact on risk stratification (in Chinese). J Guangxi Med Univ 2015;32:283-285.
15. Walter T, Apfaltrer P, Weilbacher F, et al. Predictive value of high-sensitivity troponin I and D-dimer assays for adverse outcome in patients with acute pulmonary embolism. Exp Ther Med 2013;5:1508-1514. https://doi.org/10.3892/etm.2012.825
16. Zhang J, Liu G, Wang S, et, al. The electrocardiographic characteristics of an acute embolism in the pulmonary trunk and the main pulmonary arteries. Am J Emerg Med 2016;34:212-217. https://doi.org/10.1016/j.ajem.2015.10.028
17. Li Q, Wang DZ, Chen BX. Electrocardiogram in patients with acute inferior myocardial infarction due to occlusion of circumflex artery. Medicine (Baltimore). 2017; 96: e6095. https://doi.org/10.1097/MD.0000000000006095
18. Winkles JA.The TWEAK -Fn14 cytokine -receptor axis: discovery, biology and therapeutic targeting. Nat Rev Drug Discov 2008;7(5): 411-425. https://doi.org/10.1038/nrd2488